

Energy-efficient tunable silicon photonic micro-resonator with graphene transparent nano-heaters

Longhai Yu¹, Yaocheng Shi¹, Daoxin Dai^{1, *} and Sailing He^{1, 2, *}

¹Centre for Optical and Electromagnetic Research, JORCEP, State Key Laboratory for Modern Optical Instrumentation, Zhejiang Provincial Key Laboratory for Sensing Technologies, Zhejiang University, Zijingang Campus, Hangzhou 310058, China.

²Department of Electromagnetic Engineering, School of Electrical Engineering, Royal Institute of Technology, S-100 44 Stockholm, Sweden.

*E-mail: dxdai@zju.edu.cn, sailing@kth.se

Abstract: Thermally-tuning silicon micro-cavities are versatile and beneficial elements in low-cost large-scale photonic integrated circuits (PICs). Traditional metal heaters used for thermal tuning in silicon micro-cavities usually need a thick SiO₂ upper-cladding layer, which will introduce some disadvantages including low response speed, low heating efficiency, low achievable temperature and complicated fabrication processes. In this paper, we propose and experimentally demonstrate thermally-tuning silicon micro-disk resonators by introducing graphene transparent nano-heaters, which contacts the silicon core directly without any isolator layer. This makes the graphene transparent nano-heater potentially to have excellent performances in terms of the heating efficiency, the temporal response and the achievable temperature. It is also shown that the graphene nano-heater is convenient to be used in ultrasmall photonic integrated devices due to the single-atom thickness and excellent flexibility of graphene. Both experiments and simulations imply that the present graphene transparent nano-heater is promising for thermally-tuning nanophotonic integrated devices for e.g. optical modulating, optical filtering/switching, etc.

Keywords: graphene; transparent nano-heater; silicon micro-disk resonator; thermal tuning

1. Introduction

Silicon photonics is one of the most promising technologies to realize low-cost large-scale

photonic integrated circuits (PICs) because of the ability for ultra-sharp bends and the compatibility with CMOS fabrication processes.^{1,2} Among various silicon photonic integrated devices, an optical micro-cavity is well known as a versatile element to realize many functionality components, including optical filters/switches,^{3, 4} optical modulators⁵ and optical sensors.⁶ Since silicon has a large heat conductivity ($\sim 149\text{W/m}\cdot\text{K}$) and a large thermo-optical (TO) coefficient ($\sim 1.8\times 10^{-4}/\text{K}$ at the wavelength of $1.55\mu\text{m}$),⁷ it is possible and beneficial to achieve efficient thermal tuning in silicon micro-cavities. Traditionally, metal heaters are usually used for thermally tuning silicon micro-cavities, and a thick SiO_2 upper-cladding layer is required between the metal heater and the silicon core to isolate metal absorption. However, this thick SiO_2 upper-cladding layer will introduce some disadvantages due to its poor heat conductivity, e.g., low response speed, low heating efficiency and low temperature increase. Moreover, silicon micro-cavities are desired to have small size for large-scale integration, in which case the fabrication becomes difficult for traditional metal heaters. Therefore, a novel and efficient heating approach for thermally-tuning silicon micro-cavities are desired very much.

Graphene has been extensively investigated all over the world because this two-dimensional (2D) sheet has many extraordinary properties,^{8, 9, 10} such as 0.34nm -thickness for monolayer graphene,¹¹ broadband absorption of $\sim 2.3\%$ per layer for vertically incident light,^{8,9} carrier mobility as high as $200,000\text{cm}^2/\text{V}\cdot\text{s}$ at room temperature (RT),^{12, 13} a “minimum” conductivity of $\sim 4e^2/h$ even when the carrier concentration tends to zero,^{8, 10} a high value of optical damage threshold and excellent mechanical stability.⁹ Recent studies also suggest that graphene is expected to have high intrinsic thermal conductivity owing to the long-wavelength phonon transport in its 2D crystal lattices,^{14, 15} and an experiment value of up to $5300\text{W/m}\cdot\text{K}$ at RT has confirmed this conclusion.¹⁶ Excellent thermal property of graphene coupled with its remarkable optoelectronic properties enables many potential applications of graphene in thermal management,^{17, 18} such as efficient heat spreaders in electronic and photonic devices,^{19, 20} transparent and flexible heaters,^{21, 22, 23} etc.^{24, 25}

In this paper, we experimentally demonstrate a thermally-tuning silicon micro-disk resonator with graphene transparent nano-heaters for the first time. The graphene

nano-heater is designed to contact the silicon core directly without the thick SiO₂ upper-cladding layer required for traditional metal heaters, which makes it possible to achieve efficient thermal tuning, high temporal response as well as simple fabrication processes. Due to the single-atom thickness and excellent flexibility of graphene, it is convenient for the transparent nano-heater to be patterned in a nano-scale shape with CMOS-compatible fabrication processes. This is very useful to small-size nanophotonic integrated devices that need thermal management, i.e., the thermally-tuning micro-disk resonator in our case. Here we characterize the thermally-tuning micro-disk resonator through a series of experiments and simulations, and show that the graphene transparent nano-heater is a novel, beneficial and promising heating method for nanophotonic integrated circuits.

2. Materials and Methods

The three-dimensional (3D) schematic illustration of the thermally-tuning silicon micro-disk with a graphene transparent nano-heater is shown in Figure 1a. The fabrication starts with a commercial SOI wafer with a 250nm-thick top silicon layer and a SiO₂ buried oxide (BOX) layer of 3 μ m. We use electron beam lithography (EBL) and inductive coupling plasma (ICP) etching processes to form the submicron-patterns. Then a second EBL process and a lift-off process are carried out to make a couple of 100nm-thick titanium metal contacts on top of the SiO₂ BOX layer. A monolayer graphene sheet, grown by chemical vapor deposition (CVD) method, is wet-transferred onto the whole SOI chip without any alignment.^{26, 27} A third EBL process followed by an oxygen plasma etching process is then utilized to pattern the graphene sheet forming the nano-heater as well as the connecting bridges that connect the nano-heater and the metal contacts.²⁶ As shown in Figure 1b, the graphene nano-heater has an annulus part on the micro-disk and two straight parts extending out of the micro-disk. The radii of the micro-disk and the annulus nano-heater are about $r_d=5\mu$ m and $r_h=3.4\mu$ m respectively. And the widths of the graphene nano-heater are about $w_h=1.2\mu$ m for the annulus part and $w_{ch}=2\mu$ m for the straight part. These designing parameters are used to keep the annulus graphene nano-heater being laid outside the region of the whispering-gallery mode (WGM) of the micro-disk resonator (see the bottom of Figure

1b),²⁸ which avoids introducing extra loss by the graphene sheet on the silicon core. Thus a transparent nano-heater is achieved.

Figure 1c shows the microscope images of the fabricated thermally-tuning silicon micro-disk resonators. To protect the patterned graphene from damage or contamination, the photoresist for patterning is not removed during the experiment. Since the guided mode is mainly confined to the silicon core (see the bottom of Figure 1b), the remaining photoresist on the graphene sheet will not influence thermal behaviors of the devices notably.²³ In Figure 1d, we show the scanning electron microscope (SEM) images of the micro-disk resonator covered by the patterned graphene nano-heater. It can be seen that the graphene sheet flexibly crosses the step from the top surface of the SiO₂ BOX layer to that of the silicon core. Therefore, the present graphene nano-heater is available for complex surfaces with non-planar nanostructures even though there is no SiO₂ upper-cladding layer.

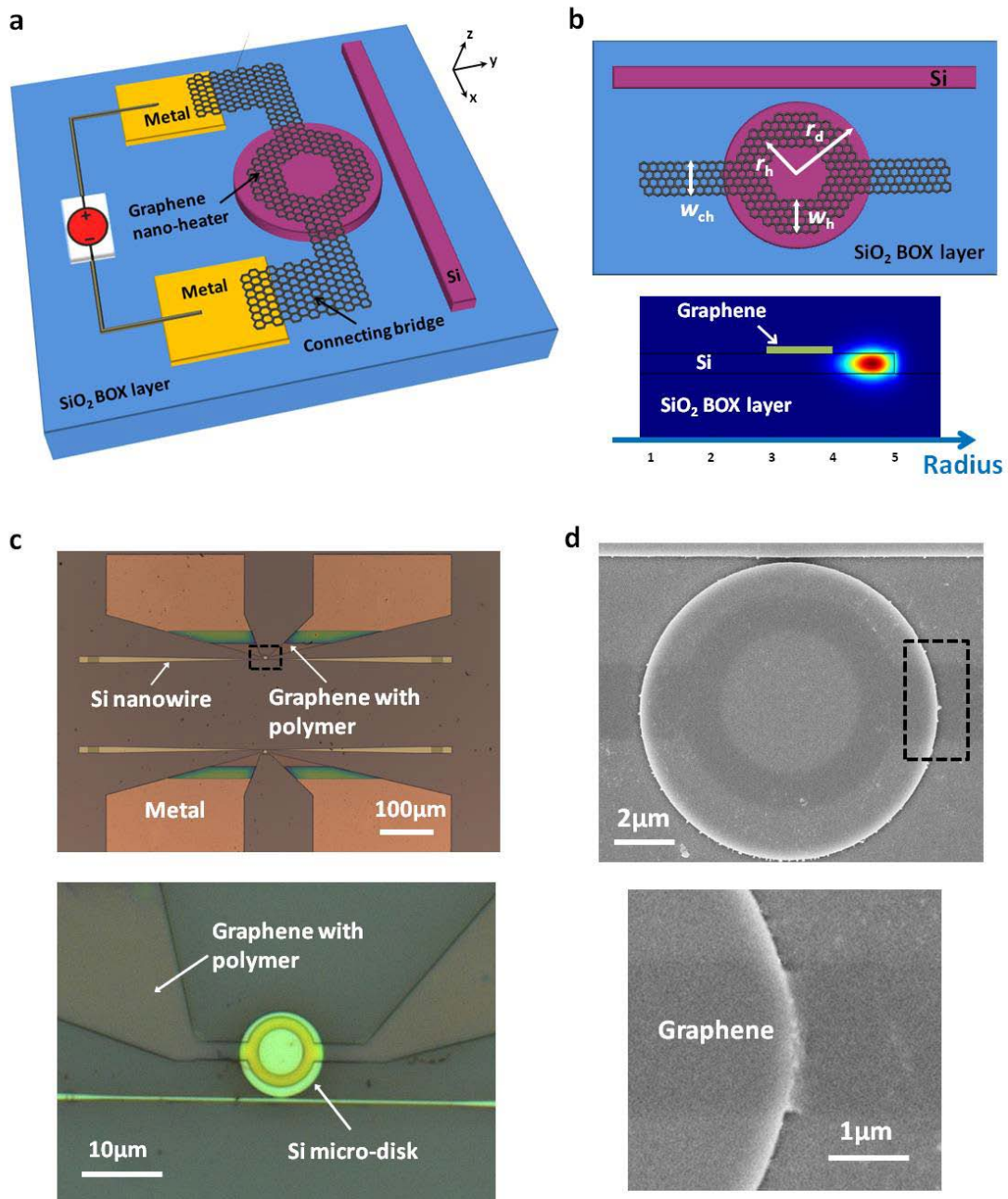


Figure 1 Thermally-tuning silicon micro-disk resonator with a graphene transparent nano-heater. **(a)** Three-dimensional schematic illustration of a thermally-tuning silicon micro-disk with a graphene transparent nano-heater. The graphene nano-heater has an annulus part on the micro-disk and two straight parts extending out of the micro-disk. The polymer on the graphene is not shown. **(b)** Top, top view for the micro-disk resonator with a graphene nano-heater. The radii of the micro-disk and the annulus nano-heater are about $r_d=5\mu\text{m}$ and $r_h=3.4\mu\text{m}$ respectively. The widths of the graphene nano-heater are about $w_h=1.2\mu\text{m}$ for the annulus part and $w_{ch}=2\mu\text{m}$ for the straight part. Bottom, cross-section view for the whispering-gallery mode (WGM) of the micro-disk resonator. The annulus

graphene nano-heater on the micro-disk is shown in a green line. **(c)** Top, top-view microscope image of the fabricated thermally-tuning micro-disk resonator (Scale bar: 100 μ m). Bottom, zoom-in view for the black dash square in the top image (Scale bar: 10 μ m). The graphene sheet is covered by a polymer film. **(d)** Top, top-view scanning electron microscope (SEM) image of the micro-disk resonator covered by the patterned graphene nano-heater (Scale bar: 2 μ m). Bottom, zoom-in view for the black dash square in the top image (Scale bar: 1 μ m). The graphene sheet flexibly crosses the step from the top surface of the SiO₂ BOX layer to that of the silicon core. The polymer on the graphene sheet is removed.

3. Results and Discussion

As is well known, the spectral response of a micro-disk resonator can be described as²⁹

$$P_{\text{out}}(\lambda) = P_{\text{in}} \left[\frac{t - e^{-i2\pi r_d \left(\frac{2\pi n_e}{\lambda} - \alpha \right)}}{1 - te^{-i2\pi r_d \left(\frac{2\pi n_e}{\lambda} - \alpha \right)}} \right]^2, \quad (1)$$

where P_{in} and P_{out} are the input and output powers, λ is the wavelength of the probe light, t is the transmission ratio in the coupling region of the micro-disk, α is the attenuation coefficient, and n_e is the effective refractive index of the WGM. For the thermally-tuning micro-disk resonator in our case, when a heating power is loaded in the graphene sheet through the two metal contacts, heat will be generated in the graphene nano-heater because of the large resistance in this region. The heat is then transferred directly from the graphene nano-heater to the silicon micro-disk below, and this causes the temperature increase of the silicon. Due to the positive TO coefficient of silicon (i.e., $\sim 1.8 \times 10^{-4}/\text{K}$), the effective refractive index of the micro-disk resonator n_e increases. As indicated in Equation (1), a phase variation is then introduced in the resonator, and consequently the spectral response of the micro-disk has a redshift thermally.

Figure 2a shows the experiment result for the dynamic spectral responses of our fabricated thermally-tuning micro-disk resonator. The resonant wavelength of the micro-disk resonator has a redshift of $\sim 5\text{nm}$ when the heating power P_{heating} varies from 0mW to 10.5mW. Then the heating efficiency, which is defined as the shift of the resonant wavelength with unit heating-power consumption, can be obtained as about $\eta_d = 0.474\text{nm/mW}$. This value indicates the conversion efficiency from the electrical heating

power to the temperature change of the silicon micro-disk, which includes a series of processes, e.g., heat generation in the graphene nano-heater, heat transfer from the graphene sheet to the silicon core, and heat delivery in the 5 μm -radius micro-disk. The temporal response of the thermally-tuning micro-disk resonator is also measured. We can get the 90% rising and decaying times of thermal tuning are $\sim 12.8\mu\text{s}$ and $\sim 8.8\mu\text{s}$ respectively. In our device, the graphene nano-heater contacts directly with the silicon core, so the time for heat transfer from graphene to silicon can be neglected, and the temporal response here mainly depends on the heat delivery in the silicon micro-disk.

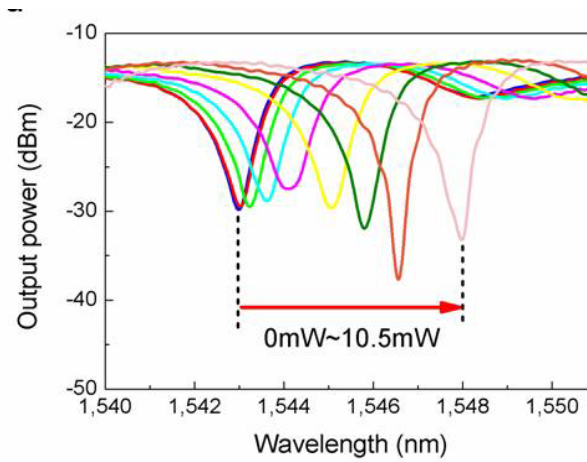


Figure 2 Spectral responses of the thermally-tuning micro-disk resonator as the heating power P_{heating} varies from 0mW to 10.5mW. The heating efficiency is about $\eta_d=0.474\text{nm/mW}$.

In order to simulate the thermal behaviors of the present thermally-tuning micro-disk resonator, we use a 3D finite element method (FEM) tool to solve the Poisson Equation. In the simulation, we assume that the electrical energy for heating is completely converted to thermal energy, and the thermal energy is distributed averagely in the graphene nano-heater. When the heating power in unit area of the graphene nano-heater is about $\sim 0.2\text{mW}/\mu\text{m}^2$, we can obtain the temperature distribution of the silicon micro-disk resonator in Figure 3a. It shows that the regions around the graphene nano-heater have higher temperature than the regions far away from the graphene nano-heater, and the highest temperature (i.e., $\sim 431.8\text{K}$) appears in the connecting regions of the annulus and straight nano-heaters. To see clearly the heat delivery in the heated micro-disk, we show the x, y and z components of the total heat flux in Figure 3b-3d. The figures indicate that the shape of the graphene

nano-heater (i.e., w_{ch} , w_h and r_h) influences the result significantly, and it is possible to increase the heating efficiency by further optimizing the shape (see below). In our device, the annulus graphene nano-heater is designed to be just near the guided mode (WGM) around the micro-disk resonator (see the bottom of Figure 1b). This is helpful to realize an efficient increase for the effective refractive index of the WGM even though the temperature distribution is not average in the heated micro-disk.

To derive a theoretical heating efficiency, we can calculate the effective temperature and the corresponding effective refractive index n_e for the WGM according to its field distribution in the micro-disk (see the bottom of Figure 1b). Then by using Equation (1), the spectral response of the micro-disk is obtained, and the theoretical heating efficiency can be derived as about $\eta_t=1.25\text{nm/mW}$. This value is higher than the measurement result in our experiment (i.e., $\sim 0.474\text{nm/mW}$). The main reason is because the conversion efficiency from the electrical energy for heating to the thermal energy in the graphene nano-heater can never be ideally 100%. The heat generated in the graphene nano-heater is not only transferred to the silicon core but also delivered to the connecting bridges due to the high intrinsic heat conductivity of graphene.¹⁶ Then the thermal energy in the connecting bridges will be wasted to heat the SiO₂ BOX layer below them. Therefore, the assumption in the simulation cannot be realized in our experiment. Another reason is the quality degradation of the graphene sheet during the fabrication process. It is observed that the wet-transferred graphene sheet has some contamination and cracks, which affects the heat transfer from graphene to silicon and reduces the heating efficiency. With the simulation, we can also get the temporal response of the thermally-tuning micro-disk resonator. The theoretical 90% rising and decaying times are both $\sim 8.3\mu\text{s}$, which are slightly faster than the measurement results (i.e. $\sim 12.8\mu\text{s}$ for the rising process and $\sim 8.8\mu\text{s}$ for the decaying process). This results from the quality degradation of the graphene nano-heater as well, and the influence to the heating process (rising process) is larger than that to the cooling process (decaying process).

To make a comparison, we simulate a thermally-tuning silicon micro-disk resonator with a traditional metal heater by using the FEM tool. The metal heater has the same shape as the present graphene nano-heater, and the SiO₂ upper-cladding layer between the metal heater and the silicon core is about $\sim 1\mu\text{m}$. From the simulation, we can get the heating efficiency of

about $\eta_m=0.94\text{nm/mW}$, which is about 25% smaller than that with the graphene nano-heater (i.e. $\eta_t=1.25\text{nm/mW}$). The reduced heating efficiency for the metal heater is owing to the addition of the thick SiO_2 upper-cladding layer, which increases the heating volume significantly. The 90% rising and decaying times with the metal heater are also obtained as $\sim 12.8\mu\text{s}$. This value is about 54% longer than the result with the graphene nano-heater (i.e., $\sim 8.3\mu\text{s}$) due to the poor heat conductivity of the SiO_2 upper-cladding region. By using metal heaters, it takes some time to deliver heat from the metal to the silicon core, while this problem is removed with graphene nano-heaters because graphene nano-heaters contact the silicon directly. Furthermore, we find that the temperature of the silicon core is much lower than that of the heater (e.g., $\Delta T=T_{\text{metal}}-T_{\text{silicon}}\sim 89\text{K}$ when the heating power in unit area of metal is $\sim 0.2\text{mW}/\mu\text{m}^2$) for the case of metal heaters. In contrast, when using graphene nano-heaters, the temperature of the silicon core is almost as same as that of the heater. Therefore, graphene nano-heaters are beneficial to achieve a higher operation temperature and a larger tunable range. The comparison above implies that graphene nano-heaters are possible to achieve better performance than traditional metal heaters in terms of heating efficiency, temporal response and maximal operation temperature for thermally-tuning nanophotonic integrated devices.

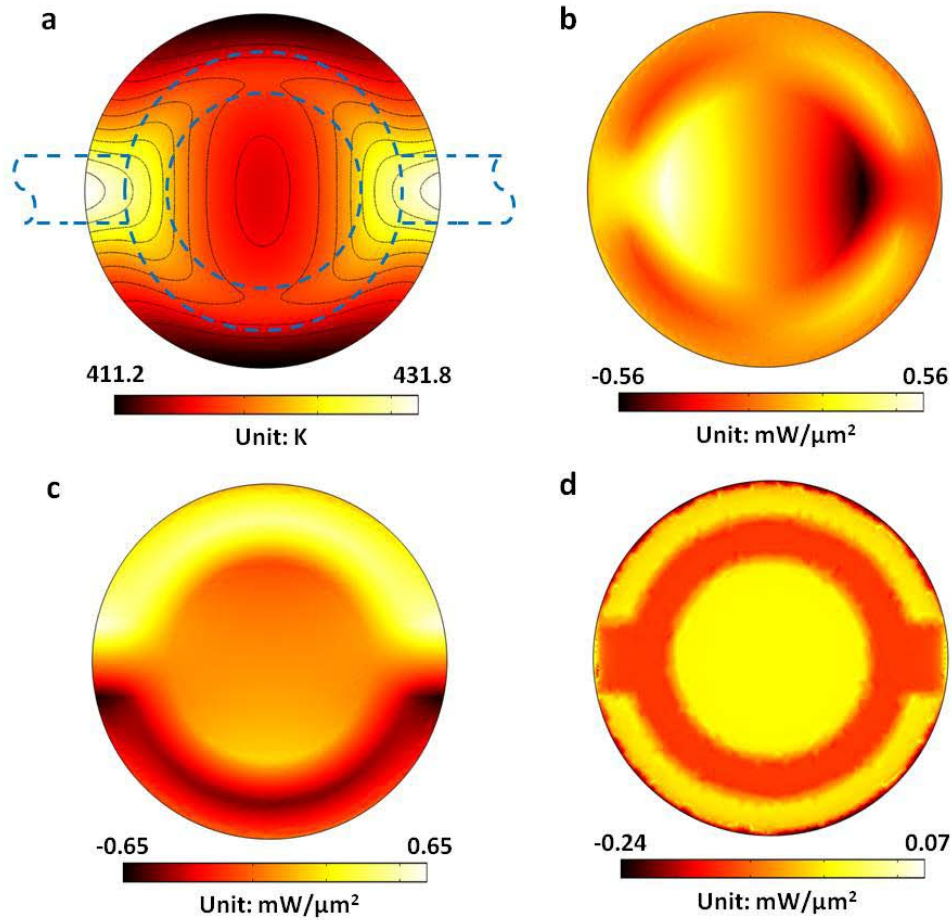


Figure 3 Simulation for the thermally-tuning micro-disk resonator with a graphene transparent nano-heater by solving the Poisson Equation with a 3D finite element method (FEM) tool. The heating power loaded in unit area of the graphene nano-heater is $\sim 0.2 \text{ mW}/\mu\text{m}^2$. **(a)** Temperature distribution of the heated micro-disk resonator. The outlines of the graphene nano-heater are shown in blue dash lines. Room temperature is 300K. **(b)** x component, **(c)** y component and **(d)** z component of the total heat flux in the heated micro-disk resonator. The coordinate axis is shown in Figure 1a.

The experiment and simulation results above have shown that the present graphene transparent nano-heater provides efficient thermal tuning for silicon micro-disk resonators. It is also noted that the heating efficiency and temporal response can be enhanced with great potential. First, we can adjust the shape of the graphene nano-heater to optimize the temperature distribution in the micro-disk, which is beneficial to realize higher heating efficiency and faster temporal response. For example, Figure 4 shows the heating efficiency

of the graphene nano-heater with varying widths for its annulus part (w_h) and straight part (w_{ch}). Considering the propagation loss, we keep the outer edge of the annulus graphene nano-heater (i.e., $r_h + w_h/2$ in Figure 1b) constant as $\sim 4\mu\text{m}$ for $5\mu\text{m}$ micro-disk resonator. The results of our experiment devices are shown as stars in the figure. We find that by increasing w_h and decreasing w_{ch} , the heating efficiencies can be as high as $\sim 1.55\text{nm/mW}$ for $5\mu\text{m}$ -radius thermally-tuning micro-disk resonators respectively. However, a larger w_h can reduce the resistance of the annulus graphene nano-heater and limit heat generation in this region, while a smaller w_{ch} may decrease the current damage threshold and the maximal operation current of the graphene nano-heater.³³ Therefore, there is a trade-off among the heating efficiency, resistance and maximal operation current in the process of designing the graphene nano-heater. In addition, the resistance of the graphene nano-heater can also be optimized. Reducing the contact resistance as well as increasing the resistance of the annulus part helps to cut the energy waste and achieve improved thermal tuning. What is more, the metal contacts can be placed closer to the graphene nano-heater so that the area of the graphene connecting bridges is shrunk to reduce heat spreading. The simulation shows that the thick SiO_2 BOX layer is such a large heat sink that it limits the heating efficiency significantly, especially when the straight graphene nano-heater and the connecting bridges contact the SiO_2 BOX layer directly in our case. To overcome this problem, one can suspend the graphene sheet^{6, 13} or insert a layer with low heat conductivity (e.g., polymer) between the graphene sheet and the substrate to prevent the heat from dissipating. Another important approach to improve the present heating efficiency and temporal response is to further enhance the graphene quality by optimizing the fabrication processes.

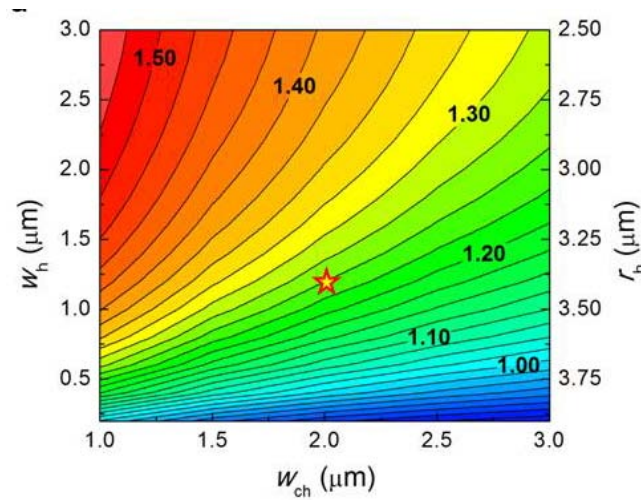


Figure 4 Theoretical heating efficiency of the thermally-tuning micro-disk resonator with a graphene transparent nano-heater. The widths of the graphene nano-heater in the straight part (w_{ch}) and annulus part (w_h) are varied. The outer edge of the annulus graphene nano-heater (i.e., $r_h + w_h/2$) keeps constant as $\sim 4\mu\text{m}$ for the $5\mu\text{m}$ -radius micro-disk resonator. The corresponding radius of the annulus nano-heater r_h is also shown. The parameters used in our experiments are indicated as stars.

4. Conclusion

In summary, a thermally-tuning silicon micro-disk resonator with a graphene transparent nano-heater is demonstrated for the first time. By optimizing the shape of the graphene nano-heater, it will introduce little extra loss even when the graphene sheet contacts directly with the silicon core. Both experiments and simulations have shown that the present graphene transparent nano-heater could achieve good performance in terms of heating efficiency, temporal response, maximal operation temperature as well as fabrication process in nano-scale devices. It is indicated that this novel heating method based on graphene has great promise for many applications in thermally-tuning nanophotonic integrated devices, such as optical modulating, optical filtering/switching and so on.

5. Acknowledgements

This work was partially supported by the National Natural Science Foundation of China (No. 91233208, 61422510), the National High Technology Research and Development Program (863) of China (No. 2012AA012201), and the Program of Zhejiang Leading Team of Science and Technology Innovation.

Reference

1. Hochberg M, Baehr-Jones T. Towards fabless silicon photonics. *Nat Photonics* 2010; **4**: 492-494.
2. Asghari M, Krishnamoorthy AV. SILICON PHOTONICS Energy-efficient communication. *Nat Photonics* 2011; **5**: 268-270.
3. Xu DX, Densmore A, Waldron P, Lapointe J, Post E, Delage A, *et al.* High bandwidth SOI photonic wire ring resonators using MMI couplers. *Opt Express* 2007; **15**: 3149-3155.
4. Almeida VR, Barrios CA, Panepucci RR, Lipson M, Foster MA, Ouzounov DG, *et al.* All-optical switching on a silicon chip. *Opt Lett* 2004; **29**: 2867-2869.
5. Xu QF, Schmidt B, Pradhan S, Lipson M. Micrometre-scale silicon electro-optic modulator. *Nature* 2005; **435**: 325-327.
6. Wang XK, Guan XW, Huang QS, Zheng JJ, Shi YC, Dai DX. Suspended ultra-small disk resonator on silicon for optical sensing. *Opt Lett* 2013; **38**: 5405-5408.
7. Espinola RL, Tsai MC, Yardley JT, Osgood RM. Fast and low-power thermo-optic switch on thin silicon-on-insulator. *Ieee Photonic Tech L* 2003; **15**: 1366-1368.
8. Bonaccorso F, Sun Z, Hasan T, Ferrari AC. Graphene photonics and optoelectronics. *Nat Photonics* 2010; **4**: 611-622.
9. Bao QL, Loh KP. Graphene Photonics, Plasmonics, and Broadband Optoelectronic Devices. *Acs Nano* 2012; **6**: 3677-3694.
10. Geim AK, Novoselov KS. The rise of graphene. *Nat Mater* 2007; **6**: 183-191.
11. Novoselov KS, Geim AK, Morozov SV, Jiang D, Zhang Y, Dubonos SV, *et al.* Electric field effect in atomically thin carbon films. *Science* 2004; **306**: 666-669.
12. Bolotin KI, Sikes KJ, Jiang Z, Klima M, Fudenberg G, Hone J, *et al.* Ultrahigh electron mobility in suspended graphene. *Solid State Commun* 2008; **146**: 351-355.
13. Du X, Skachko I, Barker A, Andrei EY. Approaching ballistic transport in suspended graphene. *Nat Nanotechnol* 2008; **3**: 491-495.
14. Balandin AA. Thermal properties of graphene and nanostructured carbon materials. *Nat Mater* 2011; **10**: 569-581.
15. Nika DL, Pokatilov EP, Askerov AS, Balandin AA. Phonon thermal conduction in graphene: Role of Umklapp and edge roughness scattering. *Phys Rev B* 2009; **79**.
16. Balandin AA, Ghosh S, Bao WZ, Calizo I, Teweldebrhan D, Miao F, *et al.* Superior thermal conductivity of single-layer graphene. *Nano Lett* 2008; **8**: 902-907.
17. Sadeghi MM, Pettes MT, Shi L. Thermal transport in graphene. *Solid State Commun* 2012; **152**: 1321-1330.
18. Ghosh S, Calizo I, Teweldebrhan D, Pokatilov EP, Nika DL, Balandin AA, *et al.* Extremely high thermal conductivity of graphene: Prospects for thermal management applications in nanoelectronic circuits. *Appl Phys Lett* 2008; **92**.
19. Subrina S, Kotchetkov D, Balandin AA. Heat Removal in Silicon-on-Insulator Integrated Circuits With Graphene Lateral Heat Spreaders. *Ieee Electr Device L* 2009; **30**: 1281-1283.
20. Prasher R. Graphene Spreads the Heat. *Science* 2010; **328**: 185-186.
21. Kang J, Kim H, Kim KS, Lee SK, Bae S, Ahn JH, *et al.* High-Performance Graphene-Based Transparent Flexible Heaters. *Nano Lett* 2011; **11**: 5154-5158.
22. Sui D, Huang Y, Huang L, Liang JJ, Ma YF, Chen YS. Flexible and Transparent Electrothermal Film

- Heaters Based on Graphene Materials. *Small* 2011; **7**: 3186-3192.
23. Yu L, He S, Zheng J, Dai D. Graphene-based Transparent Nano-heater for Thermally-tuning Silicon Nanophotonic Integrated Devices. *PIERS Proceedings*; 2014; 2014.
 24. Yang N, Zhang G, Li BW. Thermal rectification in asymmetric graphene ribbons. *Appl Phys Lett* 2009; **95**.
 25. Park SD, Lee SW, Kang S, Bang IC, Kim JH, Shin HS, *et al.* Effects of nanofluids containing graphene/graphene-oxide nanosheets on critical heat flux. *Appl Phys Lett* 2010; **97**.
 26. Yu L, Zheng J, Xu Y, Dai D, He S. Local and Non-Local Optically Induced Transparency Effects in Graphene-Silicon Hybrid Nanophotonic Integrated Circuits. *Acs Nano* 2014.
 27. Yu L, Xu Y, Shi Y, Dai D. Linear and Nonlinear Optical Absorption of on-chip Silicon-on-insulator Nanowires with Graphene. *Asia Communications and Photonics Conference*; 2012 November 7-10; Guangzhou, China; 2012. p. AS1B.3.
 28. McCall SL, Levi AFJ, Slusher RE, Pearton SJ, Logan RA. Whispering-Gallery Mode Microdisk Lasers. *Appl Phys Lett* 1992; **60**: 289-291.
 29. Bogaerts W, De Heyn P, Van Vaerenbergh T, De Vos K, Selvaraja SK, Claes T, *et al.* Silicon microring resonators. *Laser Photonics Rev* 2012; **6**: 47-73.
 30. Smith JT, Franklin AD, Farmer DB, Dimitrakopoulos CD. Reducing Contact Resistance in Graphene Devices through Contact Area Patterning. *Acs Nano* 2013; **7**: 3661-3667.
 31. Xia FN, Perebeinos V, Lin YM, Wu YQ, Avouris P. The origins and limits of metal-graphene junction resistance. *Nat Nanotechnol* 2011; **6**: 179-184.
 32. Wang L, Meric I, Huang PY, Gao Q, Gao Y, Tran H, *et al.* One-Dimensional Electrical Contact to a Two-Dimensional Material. *Science* 2013; **342**: 614-617.
 33. Murali R, Yang YX, Brenner K, Beck T, Meindl JD. Breakdown current density of graphene nanoribbons. *Appl Phys Lett* 2009; **94**.